J. Marine. Sci. Appl. (2009) 8: 323-327
DOI: 10.1007/s11804-009-8070-8

Effects of the profile of a supercavitating vehicle's front-end on supercavity generation

ZHANG Bo*, ZHANG Yu-wen and YUAN Xu-long

College of Marine Engineering, Northwestern Polytechnical University, Xi'an 710072, China

Abstract: The authors designed three different front profiles for supercavitating vehicles based on cavity theory and the Granville streamlined equation are designed. Experiments were done using these front profiles in the Northwestern Polytechnical University high-speed water tunnel. The experiments indicated that the critical volume of gas required for supercavitation is affected by the axial distribution of the front-end's slope. The experimental data showed critical gas flow rates required for the three designs were less than mod-1, with the greatest decrease 24%. The experimental results also showed the supercavitation generation speeds of the models were faster than mod-1 by up to 32.4%. This verifies that the front profile of a supercaviting vehicle effects supercavity generation speed and critical gas flow rates. The smaller the changes in axial distribution of pressure, the higher the supercavity generation speed. The smaller the changes in curvature distribution of axial, the smaller the critical gas flow rates.

Keywords: cavitation; supercavitating vehicle; volumetric gas flow rate; front profile; supercavitation generation speed

CLC number: O352 **Document code:** A **Article ID:** 1671-9433(2009)04-0323-05

1 Introduction

To our knowledge, the literature about supercavitating vehicles mainly focused on the study of the cavity generation and shape of cavity based on the number of cavities[1], cavitator[2-5] and volumetric gas flow rate. There is no paper in the published literature on the effect of the profile of supercavitating vehicle on the generation speed of a supercavity and the critical gas flow rates. After many pool and water tunnel experiments, it is found that the cavity generation and development processes have obvious stagnancy in the areas where the expansion parts of the vehicles are connected with the cylinder parts of the vehicles. It deteriorates the smooth crossing of the cavities in the connection areas, thus affects the speed of supercavitation generation. In addition, it is also found that the critical volumetric gas flow rate required for a complete supercavitation is different for different expansion part profiles.

During the process of supercavitation growing, the vehicle would change from the state enveloped with water to the supercavitation state, the fluid dynamic of the vehicle has a dramatic change. Under this condition, the movement of the vehicle is very difficult to be controlled. One solution to this problem is to improve the speed of the supercavitation generation, reducing the time of the instability state. In addition, a supercavitating vehicle is a self-contained system, the energy required for thrusting of the vehicle and generation of the ventilation gas comes from the vehicle itself. Reducing the critical ventilation flow gas can reduce the energy consumption, which is of great significance to increasing the range of the vehicle's movement for a fixed amount of total energy. Therefore, the study about the supercavitation generation speed and the critical ventilation gas flow rate is very important for the successful transition of a supercavitating vehicle from an unstable state (vehicle is partly surrounded by water) to a supercavitation state (vehicle is surrounded by gas). Currently, the main method for shortening the time of supercavitation generation is to increase the propulsion force. This is an effective way of reducing the supercavitation generation time, while in the meantime, a number of other problems and difficulties will appear. In this paper, the emphasis is mostly put on how to improve the supercavitation's growing speed and to reduce the critical ventilation gas flow rate based on the front shape of the vehicles.

2 Front profile and design methods for supercavitating vehicles

2.1 Basic shape of the supercavitating vehicle and the definition of $\overline{Q}$ (ventilation gas coefficient)

At present, the general shape of the supercavitating vehicle is shown in Fig.1. Linear expansion is usually employed to

Received date: 2008-10-22.
***Corresponding author Email:** zb994332@sina.com

design the expansion section. This is also the most popular form used in domestic and foreign studies.

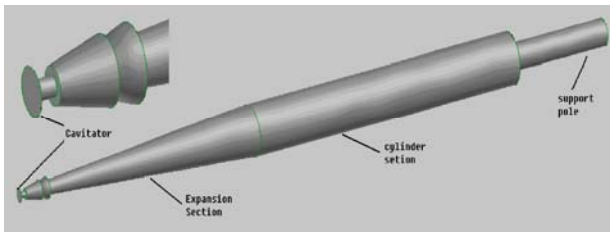

Fig.1 Scheme of the supercavitating vehicles

The main problem for the ventilated cavitation flow is the gas quantity necessary for a given number of cavities. So the non-dimensional ventilation gas coefficient[6] is introduced:

$$\bar{Q} = \frac{\dot{Q}}{V_\infty D_n^2} \tag{1}$$

where $\dot{Q}$ is the volumetric gas rate at the pressure P_c, its dimensionality is m^3/s; D_n is the cavitator diameter.

3 Front profile of supercavitating vehicles

When the supercavitating vehicle is moving, the vehicle must be enveloped by liquid. So the profile of the vehicle is always designed to be streamline. That is to say, the slop and curvature of the front profile of the vehicle must be continuous, including the boundary points. Therefore, in this paper the Granville lines expressions with two parameters[7] are employed. Considering the characteristics of the front profile of the supercavitating vehicle and previous experimental results, a series of front shapes are designed. Based on the distribution of the surface's curvature and the smoothness of the surface pressure distribution without cavity, four types of supercavitating vehicle profiles are selected and shown as follows.

3.1 Front profile equations of the vehicle

Mode 1:

$$y = (0.0699 \cdot L_Z \cdot x - 0.2011)/R \quad (0 \le x \le 1) \tag{2}$$

where L_Z is the length from the cavitator to the connection of the expansion part and the cylinder part; R is the maximum radius of supercavitating vehicle.

Mode 2:

$$y(x) = \frac{1}{2f_r}[s_t^2 f_1(x) + (\frac{1-x_m}{x_m})^2 k_1 f_2(x) + G(x)]^{\frac{1}{2}} \quad (0 \le x \le 1) \tag{3}$$

$$G(x) = x^3(6x^2 - 15x + 10)$$

$$f_1(x) = -x^2(x-1)^3$$

$$f_2(x) = -x^3(x-1)^2$$

where f_r is the slenderness ratio; s_t is the slope of intersection point of the cylinder section and the expansion section of the vehicle. The design value of s_t is 1.9996; x_m is the dimensionless coordinate of the place where the expansion section designed by the author is connected with the cylinder section; k_1 is the curvature value when x is equal to x_m, the design value is 0.5.

Mode 3:

$$y^2 = r_0 R(x) + k_{s1} K_{s1}(x) + Q(x), (0 \le x \le 1) \tag{4}$$

$$R(x) = 2x(x-1)^4$$

$$K_{s1}(x) = \frac{1}{3}x^2(x-1)^3$$

$$Q(x) = 1 - (x-1)^4(4x+1)$$

where r_0 is the curvature radius at $x = 0$. The design value of r_0 is 1; k_{s1} is the changing rate of the curvature at x=1. The design value is 28.65.

Mode 4:

$$y^2 = s^2 S(x) + k_{s1} K_{s1}(x) + Q(x), (0 \le x \le 1) \tag{5}$$

$$S(x) = x^2(x-1)^4$$

$$K_{s1}(x) = \frac{1}{3}x^3(x-1)^3$$

$$Q(x) = 1 - (x-1)^4(10x^2 + 4x + 1)$$

where s is the slope at x=0. The design value is 0.000 692; k_{s1} is the rate of curvature change at $x = 1$, the design values is 20.

3.2 Linear characteristic analysis

The CFD method is used to calculate the geometric characteristics and the pressure distribution characteristics of the four models. The results are presented and compared in Figs.2 ~ 4. Because mod1's expansion part is cone, its curvature has no change. So there is no mod1's curvature information in Fig.3.

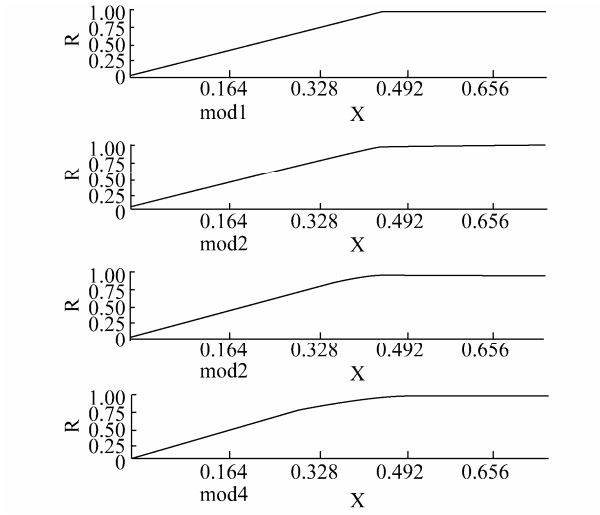

Fig.2 Four types of front part profiles

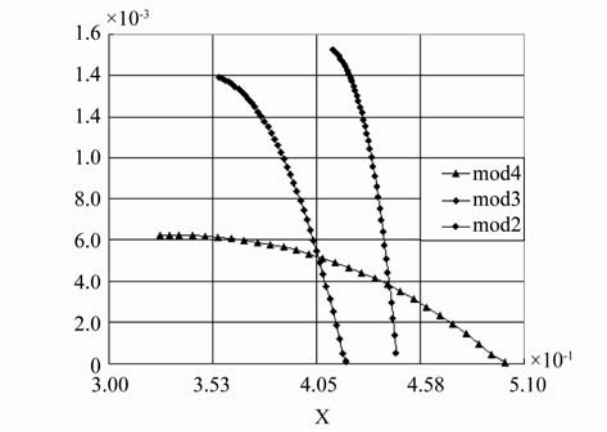

Fig.3 Slope distribution characteristics

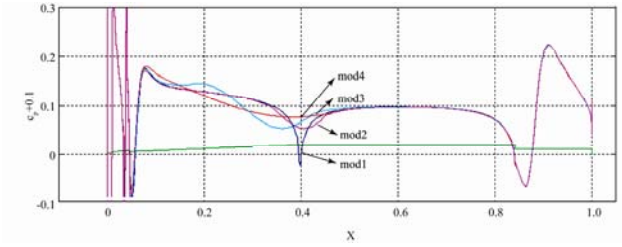

Fig.4 Characteristics of pressure distribution, when the vehicle is enveloped with water

4 Experimental results and analysis about the vehicle profile

The experimental research was carried out in the NWPU high speed water tunnel. The length of the high speed water tunnel's working section is 2m, with a cross-section diameter of 0.4 m. The water velocity is continuously adjustable from 0 ~ 18 m / s, and the hydraulic pressure is continuously adjustable from 0.01 ~ 0.3 MPa. The tunnel is equipped with water treatment systems, high-speed data acquisition systems, artificial ventilation systems and automatic monitoring and control system for the cavity pressure. The range of ventilation gas flow rate is 0 ~ 200 (L / min), which is continuously adjustable and the precision is 0.5%. The measurement range of cavity pressure is 0 ~ 10 kPa and the precision is 0.5 %. The frequency of the high-speed video on is 24 to 100 frame/second.

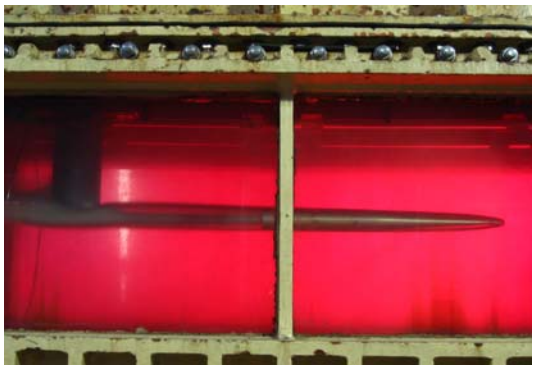

Fig.5 Model installation

Based on the four models mentioned above in this paper, four types of experimental models are made, which have the same shape and physical dimension except for the front part profiles. The total length of these models is 900 mm, and the maximal diameter is 40 mm. All the models are made with stainless steel. In order to reduce the interference of the support equipment, the models are fixed at the tail. The model installation in the tunnel is shown in Fig. 5.

4.1 Analysis and comparison of the influences of the vehicle's front shape on the cavity generation speed

Experiments for every model must be done under the same experimental condition. Based on the experience and the data of the prior water tunnel experiments on supercavitation, in this experiment, the ventilated cavity number is chosen as $\sigma_c = 0.08$, which is realized by regulating the natural cavity number and the ventilated gas flow. The expected nature cavity number can be achieved by adjusting the pressure and speed of the water tunnel. The ventilated gas flow rate can be controlled by the automatic control system of the ventilating device.

In order to study the influence of the ventilated gas flow rate on the cavity generation speed, two kinds of experimental conditions with different ventilation flow rates were designed in the experiments.

The first experimental condition:

$\sigma_v = 1.4787$, $\bar{Q} = 0.0074$, $\sigma_c = 0.08$;

The second experimental condition:

$\sigma_v = 1.9414$, $\bar{Q} = 0.0148$, $\sigma_c = 0.08$.

Notice: the parameters V_∞ and P_∞ have the same value for different models when the parameters σ_V and $\bar{Q}$ are the same.

The experimental results are given in Table 1. The data indicates the time needed for cavity generation of all the three models designed in this paper is shorter than mod1. The time of mod2 is close to mod3, and the time of mod4 is minimal in the four models. The maximum reduction ratio is as much as 33.6 percent in comparison with mod1. Considering Figs. 3 and 4, it can be seen that the time required for generating cavity is shorter for a front part with smoother axial pressure and curvature distribution.

In addition, if the cavity number is fixed, the larger the ventilation flow rate, the less the blockage during the cavity development, and it is more effective to reduce the generation time. The data from of the experiments with two kinds of conditions illustrate that although the cavity generation time is different, the trend is basically the same.

Table 1 Time required for supercavitation generation

	conditions			
	$\sigma_v = 1.478$, $\bar{Q} = 0.0074$		$\sigma_v = 1.941$, $\bar{Q} = 0.0148$	
model	$T(s)$	$\frac{T_{\mathrm{mod1}} - T_{\mathrm{mod}\,x}}{T_{\mathrm{mod1}}}(\%)$	$T(s)$	$\frac{T_{\mathrm{mod1}} - T_{\mathrm{mod}\,x}}{T_{\mathrm{mod1}}}(\%)$
mod1	1.82	0.0	1.05	0.0
mod2	1.57	13.7	0.85	19.0
mod3	1.60	12.1	0.84	20.0
mod4	1.42	21.9	0.71	32.4

4.2 Analysis and comparison of the influence of the front shape of the vehicle on the critical volumetric gas flow rate

These experiments with different models must be carried out under the same condition and this condition can guarantee the production of supercavitation. Based on the prior experimental data and experience, the conditions are chosen as follows in this experiment: D_n =10 mm , V_∞ =9~12 m/s, σ_c = 0.05~0.08. The ventilated cavity number can be adjusted by controlling the pressure of the water tunnel's working section and velocity of the tunnel's flow water. The ventilated flow rate can be controlled by the automatic monitoring and control system. During the experiment, the water speed is fixed.

The experiments are carried out under the following conditions.

1) D_n = 10 mm, V_∞ = 11 m/s, P_∞ =0.092 MPa;

2) D_n = 10 mm, V_∞ = 11 m/s, P_∞ =0.06 MPa;

3) D_n = 10 mm, V_∞ = 11 m/s, P_∞ =0.05 Mpa;

4) D_n = 10 mm, V_∞ = 11 m/s, P_∞ =0.039 Mpa;

5) D_n = 10 mm, V_∞ = 11 m/s, P_∞ =0.027 Mpa.

Table 2 Coefficient of critical ventilated gas flow rate

mod1		mod2		mod3		mod4	
σ_C	$\bar{Q}_m$	σ_C	$\bar{Q}_m$	σ_C	$\bar{Q}_m$	σ_C	$\bar{Q}_m$
0.051	0.359	0.051	0.348	0.051	0.321	0.051	0.301
0.053	0.290	0.055	0.223	0.054	0.232	0.054	0.203
0.057	0.186	0.057	0.167	0.057	0.167	0.058	0.140
0.062	0.115	0.063	0.095	0.063	0.097	0.062	0.100
0.066	0.095	0.069	0.080	0.069	0.076	0.070	0.060

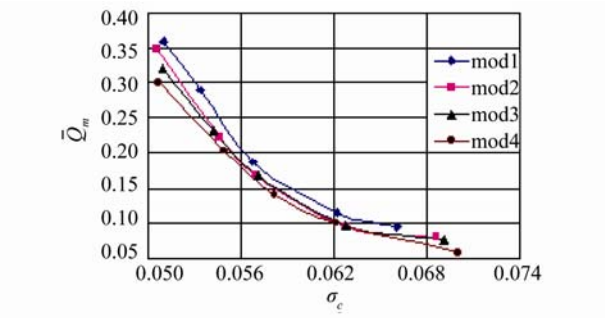

Fig.6 Trend of the critical ventilation flow coefficient for different experiment conditions

The data of the critical ventilation gas flow rate from the experiments are shown in Table 2. The trend of the critical ventilation gas change with different σ_c is shown in Fig.6. It is shown that under the same test condition, the critical ventilated gas flow rate required for the vehicles designed by the authors is significantly less in comparison with mod1, especially mod4. Fig. 3 shows that if the curvature distribution is smoother, the critical ventilation gas needed for the supercavitation will be less. According to the data of the experiments under five different conditions, it is observed that the trends of change are the same.

Based on the data shown in Table 2, the average percentages of reduction in the ventilation gas flow rate of the designed models in this paper, compared with mod1, are shown in Table 3.

Table 3 Decrease percent of the designed models compared with mod1

$\frac{(\bar{Q}_{\mathrm{m1}} - \bar{Q}_{\mathrm{m2}})}{\bar{Q}_{\mathrm{m1}}}/\%$	$\frac{(\bar{Q}_{\mathrm{m1}} - \bar{Q}_{\mathrm{m3}})}{\bar{Q}_{\mathrm{m1}}}/\%$	$\frac{(\bar{Q}_{\mathrm{m1}} - \bar{Q}_{\mathrm{m4}})}{\bar{Q}_{\mathrm{m1}}}/\%$
4	15	24

The experiments indicate that the extent of the influence of the vehicle's front part profile on the critical volumetric gas flow rate required for supercavitation generation is affected by the axial distribution of the front part's slope. For a smaller slope, the critical volumetric gas flow rate is less. Critical gas rate necessary for the three modes designed by

the authors is less than mod1, and the maximal decrease is up to 24%.

5 Conclusion

Through analysis of experimental data about supercavitation generation, some general conclusions can be drawn:

1) Supercavitation generation speed is affected by the front profile of the supercavitating vehicle, especially the axial pressure and the slope distribution of the front profile. If the change rate of the front profile's pressure distribution is smaller, the supercavitation generation speed will be slower. The results of the experiments illuminate that supercavitation generation speed of the three modes designed by the authors is faster than mod1.

2) The critical volumetric gas flow rate required for supercavitation generation is also affected by the axial distribution of the front profile's slope. For a smaller change in slope distribution, the critical volumetric gas flow rate is less.

3) Granville equation is eligible for supercavitating vehicle's profile design, the application is also convenient.

References:

[1] SEMENENKO Vladimir. Artificial supercavitation. physics and calculation. RTO AVT/VKI special course: supercavitating flows, von Karman Institute for fluid dynamics[R]. Rhode-Saint-Genese, Belgium, 2001: 12–16.

[2] WAID R L. Cavity shapes for circular disks at angles of aAttack[R]. CIT Hyd. Rpt. E-73. 4, 1957.

[3] CHOI J H, PENMETSA R C, VGRANDHI R. Shape optimization of the cavitator for a supercavitating torpedo[J]. Struct Multidisc Optim, 2005, 29: 159-167.

[4] JIA Liping, WANGCong, YU Kaiping, et al. Experimental investigation of cavitator parameters[J]. Engineering Mechanics, 2007, 24(3): 159-164.

[5] WANG Haibin, ZHANG Jiazhong, WEI Yingjie, et al. Study on relations between cavity form and typical cavitator parameters[J]. Journal of Hydrodynamics, 2005 20(2): 251-258.

[6] ZHANG Yuwen. Cavity theory and application[M]. Xi'an: Northwestern Polytechnical University Press, 2007.

[7] GRANVILLE P S. Geometrical characteristics of streamlined shapes[J]. Journal of Ship Rasearch, 1969, 13(4): .

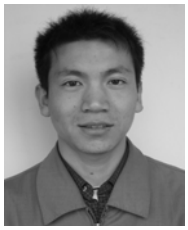

Zhang Bo was born in 1979. He is a PhD candidate at Northwestern Polytechnical University, majoring in weapon firing theory and technology.

Zhang Yu-wen was born in July 1946. He is a professor and doctoral supervisor at Northwestern Polytechnical University, majoring in weapon system and expert engineering, firing theory and technology, trajectory and control, etc.

Yuan Xu-long was born in 1977. He is an instructor at Northwestern Polytechnical University, majoring in firing theory and technology, trajectory and control, etc.

超空泡航行体前部线型对空泡生成过程的影响

张博，张宇文，袁绪龙

(西北工业大学 航海学院，陕西 西安 710072)

摘　要：本文基于航行体超空泡理论和格兰威尔线型设计方法，设计了三种具有不同前部线型的航行体模型. 并针对所设计的三种模型和具有锥形前部外型的航行体模型在西北工业大学水洞中进行了前部线形对超空泡生成影响的实验研究. 结果表明：超空泡生成速度和空泡成生所需临界通气量与航行体的轴向斜率分布有关，模型表面斜率轴向分布曲线越平坦或变化率越小，越有利于提高空泡的生成速度、减少超空泡生成所需的临界通气量. 实验数据显示文中设计的三种格兰威尔前部线型航行体与锥形前部外型航行体相比，生成超空泡所需临界通气量都有明显减小，空泡生成速度有明显提高. 文章研究方法为降低超高速航行体超空泡生成所需的临界通气量，提高空泡的生成速度提供了一条技术途径和研究方法.

关键词：超空泡航行体；线型设计；临界通气量；前部线型；超空泡生成速度